

## Scale-up of continuous microcapsule production

Sven R. L. Gobert<sup>a\*</sup>, Simon Kuhn<sup>b</sup>, Roberto F. A. Teixeira<sup>c</sup>, Leen Braeken<sup>a,b</sup>, Leen C. J. Thomassen<sup>a,b</sup>

<sup>a</sup>KU Leuven, Department of Chemical Engineering, Sustainable Chemical Process Technology TC, Diepenbeek Campus, Research unit CIPT, Diepenbeek, Belgium

<sup>b</sup>KU Leuven Department of Chemical Engineering, Leuven, Belgium

<sup>c</sup>R&D, Devan Chemicals, Ronse, Belgium

\*Corresponding author. Tel.: +321180336. E-mail: sven.gobert@kuleuven.be (S.R.L. Gobert).

Keywords: inline rotor stator mixer; scale-up; continuous emulsification; microencapsulation

### Abstract

The objective of this work is to establish an experimental approach to scale up the production of microcapsules in an inline rotor stator mixer (RSM), ensuring product size distributions as developed in batch. The emulsification step for a melamine formaldehyde microencapsulation process is therefore studied in a lab scale batch and an inline pilot scale RSM. The inline RSM is operated in CSTR mode, seldom reported in literature, allowing any feed flow rate to be implemented ranging from lab scale to (pilot) production scale (4-330 ml/min). Parameters including the Weber number, tip speed and energy density are investigated to correlate the mean capsule size of the batch and flow process. As a model system, silicone oil is dispersed in melamine formaldehyde prepolymer by the RSM at a high oil-to-water ratio of 46%. Rotational speeds range from 3000-26000 rpm. Volume based capsule size distributions presented no common correlating parameter, however the dimensionless maximum diameter correlated well with the Weber number to the power -0.4, for both devices operated at the same residence time. The difference in mean diameter and covariance between batch and flow at similar weber numbers is attributed to differences in droplet break-up mechanism due to different rotor stator geometries. Volume and number based mean diameters showed little influence of the feed flow rate of the CSTR operated inline RSM, making it an ideal tool to experiment on lab scale and increase production by increasing the feed flow rate, while maintaining rotor-stator geometry.

### 1 Introduction

Microencapsulation is the process of enveloping an active ingredient into a shell. The process of microencapsulation begins with the generation of an emulsion, which acts as a capsule template, the end product being a spherical particle with a liquid core and a hard protective shell (Bansode et al., 2012; Martin-Banderas et al., 2010; Singh et al., 2010). Lab scale development of microencapsulation processes is almost exclusively performed in batch whereby a batch operated rotor stator mixers is used to generate fine emulsions (Håkansson and Innings, 2017). They operate by high speed rotation ( $20 - 100 \text{ s}^{-1}$ ) of a rotor within a stator, separated by the shear gap (Håkansson, 2018). The centrifugal force induced by the rotor pushes the liquid through slots of the stator forming jets. The liquid is also subjected to high shear forces between the rotor and the stator (Cohen et al., 2005).

Apart from batch processing, the RSM can be used in different modes of operation, including semi batch and inline. Inline operation is especially gaining interest at production scale, because of the economic benefit of continuous operation (Håkansson and Innings, 2017). Transition from batch scale to process scale will thus require a change in mode of operation (John 2019). Furthermore equipment size (rotor diameter) and geometry (rotor stator design) can also change from batch to inline devices, which could alter the emulsification process. Therefore scaling parameters should also be considered. Several considerations (mode of operation, residence time, flow fields and scaling) of this batch to flow transfer and scale-up are discussed in the following section of the introduction.

### 1.1 Mode of operation: batch to flow conversion

A rotor stator mixer (RSM) is operated in batch mode by placing it in a tank. Turbulent circulating streams are present over the entire tank volume, as liquid is drawn into the rotor zone and expelled through the stator slots. To transform it to an inline operating mode, a flow cell with an inlet and outlet needs to encase the rotor stator head. This will enable the mixer to function as a centrifugal pump and be implemented in continuous or batch processing. Continuous processing entails a single pass system, while in batch processing the inline RSM recirculates a certain tank volume for a set operating time. The mode of operation (inline or batch) has a strong influence on the power draw, the turbulent flow fields and the number of turnovers, all of which influence emulsification efficiency (Cohen et al., 2005; Håkansson et al., 2017).

#### 1.1.1 Power draw

Power draw indicates the amount of energy the rotor delivers to the liquid. In a batch RSM the power consumption is described by

$$P_T = P_{O_z} \rho N^3 D^5 + P_L \quad (1)$$

$P_T$  is the rotational energy needed to overcome liquid resistance,  $P_{O_z}$  is the power number when no flow is passing the rotor stator and  $P_L$  are energy losses due to friction in the bearings of the rotor.  $\rho$  ( $\text{kg/m}^3$ ) is the liquid density,  $N$  ( $\text{s}^{-1}$ ) the rotational speed and  $D$  (m) the rotor diameter. However with an inline RSM the pumping action induced by the rotor resulting in a flow through the RSM is taken into account by a separate term,  $P_F$ , which represents the power needed to accelerate the liquid entering the mixing chamber to the tip speed. It is proportional to the kinetic energy of the liquid,  $D^2 N^2$ . An expression for power draw of an inline rotor stator mixer was developed by Kowalski (2009) for an inline RSM (Kowalski, 2009). The total power draw is the sum of these three terms (Cooke et al., 2011; Hall et al., 2010).

$$P_{tot} = P_{O_z} \rho N^3 D^5 + k_1 \rho Q N^2 D^2 + P_L \quad (2)$$

Whereby  $Q$  is the flow through the rotor stator chamber and  $k_1$  is a dimensionless proportionality constant. This expression differs depending on the flow regime, in turbulent conditions ( $Re > 10^4$ ) the  $P_{O_z}$  is constant and independent of  $Re$ , leading to expression (4), while in the laminar regime the power number is dependent on  $Re$  as follows

$$P_{O_z} = k_0 Re \quad (3)$$

Which then allows to express the power draw in the laminar regime as

$$P_{tot} = k_0 N^2 D^3 \mu + k_1 \rho Q N^2 D^2 + P_L \quad (4)$$

Expressions 4 and 6 indicate the dependence of the powered draw on the rotational speed. A cubic dependence indicates turbulent flow while a quadratic relation indicates laminar flow. The flow regime helps to understand which forces act to break-up droplets. In the laminar regime simple shear, elongational and hyperbolic flows induce droplet break-up, they are represented by velocity gradients or shear rate,  $\dot{\gamma}$  (Pacek et al., 2013). The relation between the maximum stable droplet diameter,  $d_{max}$  and the shear rate is as follows

$$d_{max} = C_1 \dot{\gamma}^{-1} \quad (5)$$

In turbulent flow random chaotic flow induces break-up through eddies of different sizes. Velocity gradients are difficult to predict in this flow regime, therefore the maximum droplet size is related to the energy dissipation (Pacek et al., 2013).

$$d_{max} = C_2 \sigma^{0.6} \varepsilon^{-0.4} \rho_c^{-0.6} \quad (6)$$

Where  $\rho_c$  is the continuous phase density.

### 1.1.2 Flow fields

For batch and inline RSM, the flow rate through the stator gaps is correlated with the rotational speed and rotor diameter as follows

$$N_Q = Q / (ND^3) \quad (7)$$

Where  $N_Q$  is the dimensionless flow rate or flow number. For batch mode operation, the flow rate is only dependant on the mixing head geometry (rotor and stator) and rotation speed. However inline operation adds restrictions to the flow, due to the casing and resistance in the piping downstream of the outlet (Cohen et al., 2005; Håkansson, 2018). This is seen by flow numbers being an order of magnitude lower in inline rotor stator mixers (0.0003-0.08) compared to batch (0.1-0.3) (Håkansson, 2018). This difference in flow rate of the liquid being jetted out of the stator slots leads to different turbulent flow in the stator holes. Through a CFD model based study it was shown that at high  $N_Q$  values (0.08) representing batch operation, well defined jets are formed (Håkansson, 2018). It is in this zone that the highest energy dissipation is expected and will determine droplet break-up, making the stator slot diameter an important scaling parameter. At low  $N_Q$  values (0.007) the zone of highest energy dissipation is localised in the rotor stator clearance gap and as the volume dissipation is much lower compared to batch only small radial jets are formed (Håkansson and Innings, 2017). The flow behaviour can be characterised by the fill ratio  $F$ , interpreted as the percentage of high speed flow filling the stator hole and defined as the ratio of flow speed to tip speed ( $U = \pi ND$ ).

$$F = U_q / U = Q / (U A_{tot}) \quad (8)$$

Whereby  $U_q$  is the flow speed of liquid with a flow rate of  $Q$  though the total stator slot area,  $A_{tot}$ . Introduction of  $F$  into equation (2) and disregarding the power losses gives

$$P = P_{O_2} \rho N^3 D^5 (1 + F(k_1 \pi A_{tot})) / (P_{O_2} D^2) \quad (9)$$

This equation indicates that as  $F$  increases the influence of rotor speed (tangential motion) increases and at

$$F > (P_{O_2} D^2) / (k_1 \pi A_{tot}) \quad (10)$$

the tangential motion exceeds the rotational power contribution.

### 1.1.3 Residence time and number of turnovers

The number of turnovers can be regarded as the number of times the same fluid element passes the mixing zone, i.e. the zone of highest energy dissipation. This increased exposure to high shear forces reduces the mean droplet size and the spread of the droplet size distribution (Hall et al., 2013). An estimation of the number of passes for a batch system,  $N_b$ , can be derived as follows (Hall et al., 2013; Kamiya and Kaminoyama, 2010).

$$N_b = Q / V_b t \quad (11)$$

Whereby  $Q$  is the volumetric flow rate through the stator,  $V_b$  the batch volume, and  $t$  the operating time. The time the liquid spends in the mixing zone is the most relevant for droplet break-up. This mean residence time is determined as follows (Hall et al., 2013).

$$t_r = V_h / Q N_b \quad (12)$$

$V_h$ , is the volume of the mixer head, which is considered to be the rotor swept volume. If an inline RSM is used in batch processing, the number of turnovers is determined similar as in batch. In contrast to a batch mode of operation, an inline RSM used in continuous processing does not allow free recirculation of the liquid and the feed passes the mixing zone only once. The time spent in the mixing zone is short compared to batch, as it passes only once through the mixing zone, and the mixing chamber volume is small compared to the feed volume flow.

$$t_r = V_h / Q_{feed} \quad (13)$$

The number of turnovers in continuous processing can be increased by recirculating the outlet flow to the feed, which gives another possible mode of operation, the CSTR mode. Whereby the number of recirculations,  $N_{CSTR}$ , is dependent on the intrinsic flow rate related to the rotational speed ( $Q_i \sim N$ ) and the feed flow rate  $Q_{feed}$ .

$$N_{CSTR} = Q_i / Q_{feed} \quad (14)$$

$$t_r = V_h / Q_{feed} N_{CSTR} \quad (15)$$

A single CSTR is known to have a large residence time distribution, which possibly means, regarding emulsification, an increase in the spread of the droplet size distribution.

## 1.2 Scaling parameters for emulsification in an inline rotor stator mixers and droplet size correlations

The three most mentioned scaling parameters for scaling emulsification processes are Weber number, energy density and tip speed (Hall et al., 2013).

### 1.2.1 Weber number

A well-known correlation of Weber number,  $We$ , and the dimensionless Sauter mean diameter,  $D_{32}$ , for turbulent liquid-liquid dispersion is given by (Paul et al., 2004):

$$D_{32}/D = C_1 We^{-3/5} \quad (16)$$

Whereby  $D$  is the rotor diameter and  $C_1$  is a dimensionless proportionality constant. The Weber number is the ratio of disruptive force, related to energy dissipation rate and cohesive force, including only the interfacial tension.

$$We = \rho_c N^2 D^3 / \sigma \quad (17)$$

With  $\rho_c$  the liquid density of the continuous phase and  $\sigma$  the interfacial tension of the emulsion and  $N$  is the rotational speed of the rotor. This Weber theory is based on the mechanistic model of Hinze (1955), which considers droplets to break when the disruptive stresses exceed the cohesive stresses, and the Kolmogorov theory of local isotropic eddies in the turbulent inertial subrange (i.e. droplets are much smaller than the turbulent macro scale and much larger than the Kolmogorov length scale) (Hinze, 1955; Paul et al., 2004). For this equation to be valid, inviscid drops are considered with a dispersed phase volume fraction  $\phi < 0.01$  avoiding droplet coalescence and alterations in the disruptive forces due to neighbouring droplets. The Weber number is used for scaling emulsification processes (Kowalski et al., 2011; Pacek et al., 2007). The theory has been extended to more concentrated systems  $0.01 < \phi < 0.3$ , for inviscid drops by the following correction.

$$D_{32}/D = C_2 (1 + b\phi) We^{-3/5} \quad (18)$$

Whereby  $C_2$  and  $b$  are constants. In the case of high viscous drops in a dilute system, the cohesive stresses also include viscous forces resisting droplet deformation next to the surface tension (Paul et al., 2004). The equation now becomes:

$$D_{32}/D = C_3 (\rho_c / \rho_d)^{3/8} (\mu_d / \mu_c)^{3/4} Re^{-3/4} \quad (19)$$

With  $C_3$  a proportionality constant and  $\rho$  and  $\mu$  the density and dynamic viscosity with indices  $c$  and  $d$  indicating the continuous or dispersed phase, respectively. This model was able to correlate data collected from batch experiments with a Rushton turbine (Calabrese et al., 1986), for droplet viscosities  $< 500$  cp and was also implemented in turbulent flow conditions in a static mixer (Berkman and Calabrese, 1988). This model has not yet been implemented for RSMs.

### 1.2.2 Energy density

Energy density implies the amount of energy per unit of processed mass,  $E_m$ , or volume,  $E_v$ , of emulsion. Karbstein *et al.* (1995) used the energy density to evaluate droplet disruption. They presented the following relation between the Sauter mean diameter and the energy density (Karbstein and Schubert, 1995).

$$D_{32} = C_4 E_v^b = C_4 (P / (\rho Q))^b \quad (20)$$

Whereby  $Q$  is the flowrate of emulsion through the mixing zone. This equation can be written in function of the energy dissipation rate,  $\varepsilon$  and the mean residence time spent in the mixing zone,  $t_r$ .

$$D_{32} = C_5(\varepsilon t_r)^b \quad (21)$$

A value of -0.40 for b, indicates that droplet disruption is governed by inertial turbulent breakage (Karbstein and Schubert, 1995), while lower values of b near -0.75, indicate a dominant influence of turbulent shear on droplet break-up (Schubert and Engel, 2004). Hall et al. (2013) proposed to give each term of the energy density i.e. the energy dissipation, related to the intensity of disruptive forces and the mean residence time, the duration of mixing, a different exponent (x and y).

$$D_{32} = C_6 \varepsilon^x \quad (22)$$

The exponents x and y are dependent on the viscosity of the oil. This correlation could accurately predict Sauter mean diameters at equal tip speeds for three different scales of inline RSM (Hall et al., 2013).

### 1.2.3 Tip speed

El Hamouz *et al.* (2009), used tip speed as scale-up parameter for stirred vessels and James *et al.* (2017) for batch RSMs (El-hamouz et al., 2009; James et al., 2017). The correlation in its general form is presented in equation (23).

$$D_{32} = C_8 U^b \quad (23)$$

Hall *et al.* (2013) also reported tip speed as scale-up parameter, which correlated better compared to energy dissipation rate and Weber number for three geometrically similar scales of single pass inline Silverston RSMs, keeping the residence time in the mixer head constant. Similar shaped droplet size distribution curves at equal tip speeds were observed, indicating the same droplet breakup mechanism at different scales. For multiple passes (40 batch turnovers) tip speeds also showed a good correlation with the Sauter mean diameter. Furthermore correlation (24) was shown to correlate tip speed with  $D_{32}$  for geometrically similar rotor stators.

$$D_{32} = C_9 U^x t_r^y \quad (24)$$

For this correlation the total residence time in the mixer head as presented in equation (12) is used.

The current study investigates the production of highly concentrated oil in water emulsions through a continuous processing method using a RSM operated in CSTR mode. Transition parameters between a lab scale batch operated high shear mixer and the inline setup are explored. The research is performed using an industrially relevant case of melamine formaldehyde based microencapsulation process for silicone oil. It is therefore preferable to report the number mean diameter ( $D_n$ ) instead of the volume mean diameter ( $D_v$ )

$$D_n = \frac{\sum_{i=1}^n d_i}{\sum_{i=1}^n n_i} \quad (25)$$

$$D_v = \frac{\sum_{i=1}^n d_i w_i}{\sum_{i=1}^n w_i} \quad (26)$$

Whereby  $w_i$  is the weighting factor based on the ratio of capsules volume to total volume of measured capsules. A number based diameter indicates which actual size is most present in the end product, while the volume based mean diameter gives an indication on the size of capsule which

contains the majority of active ingredient (i.e. the core content). Only a few articles discuss the number based mean diameter, through  $D_{50}$  (Kamiya and Kaminoyama, 2010) or alternatively the mode of the distribution curve (Hert and Rodgers, 2017). Both volume and number distribution derived mean diameters are included in the discussion and their covariances indicated with indices  $v$  and  $n$  respectively.

## 2 Materials and methods

### 2.1 Equipment

An IKA batch rotor stator mixer (RSM), Ultra Turrax 18 G ST and an IKA magic lab inline RSM are used to generate emulsions. Both devices are classified as teeth-design RSM. The batch and inline rotor stator geometries are shown in Figure 1.

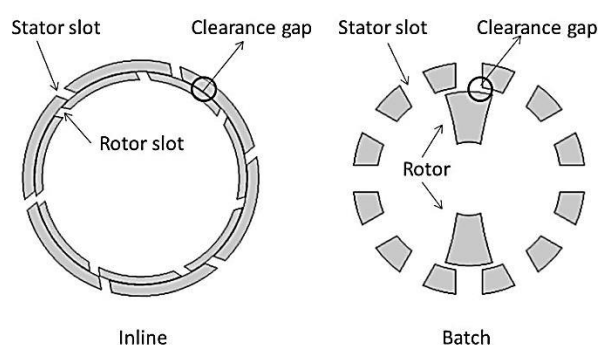


Figure 1: Rotor stator geometry of the lab scale RSM and pilot scale inline RSM.

The rotor and stator of the batch mixer have a very open design whereby the rotor has two teeth of 4 mm and the stator has 12 slots of 2.03 mm, the shear gap is 0.74 mm. In contrast the inline RSM is a very closed construction, having 7 rotor slots and 6 stator slots of 1.36mm, the shear gap is also smaller: 0.18 mm. The 18 G ST Ultra Turrax has a rotational speed range of 3000 – 25000 rpm with increments of 100 rpm. The IKA magic lab is equipped with the DR module and is operated with a single rotor stator module 2G. It can operate at 3000 up to 26000 rpm with steps of 200 rpm. The inline RSM inlet and outlet are adapted to include a temperature sensor and a recycle loop. The temperature sensor is placed in a T-piece at the original outlet of the device, Figure 2. The outlet stream is diverted to the inlet via a recycle loop. In the centre of the recycle a Y-junction is used to continuously drain part of the recirculating emulsion. Using a recycle loop allows the inline high shear mixer to operate with low feed flow rates (<10 g/min). These are far below the intrinsic flow rate determined by the pump characteristic of the RSM, which shows a minimum flow rate of 149 g/min at 3000 rpm. Without the recycle loop any feed flow rate below 137 g/min would cause cavitation, which could damage the device. The tested feed flow rates range from 4 to 330 g/min, and rotational speeds from 3000 to 26000.

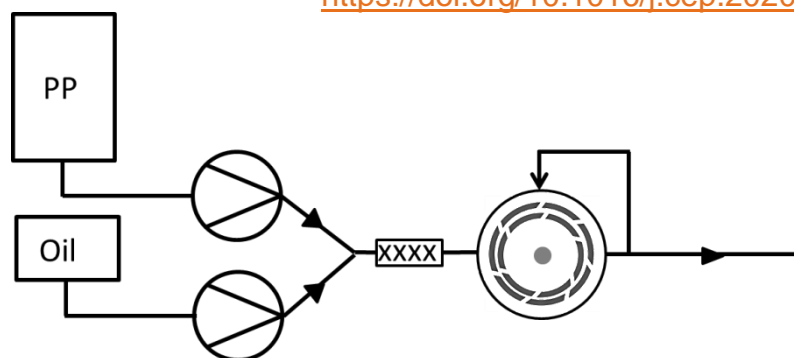


Figure 2: Schematic representation of the inline setup.

## 2.2 Pumping capacity

The intrinsic flow rate of the inline RSM is expressed as kg/s and is measured through weighted samples. To get an indication of the flow rate delivered by the batch rotor stator, a custom housing is placed around the mixing head, essentially making it an inline operated RSM. This gives an approximation of the fluid displacement rate as the housing ensures the area through which the liquid is drawn into the mixing chamber is separated from the stator slots by a rubber seal. The housing has a diameter of 2.8 cm and surrounds the RSM shaft of 1.4 cm diameter. The liquid is directed to the outlet (10 mm inner diameter) at 60 mm above the mixing head. This short distance and large exit tube diameter create minimal pressure drop and as a result the measured flow rate is considered to be the flow rate measured in almost free flow conditions.

## 2.3 Power draw of inline and batch RSM

A calorimetric measurement is used to determine the power draw, which is referred to as the dissipated power,  $P_{\text{diss}}$ . The  $P_{\text{diss}}$  of the batch RSM is determined in a Optimax reactor (Mettler Toledo) with a reactor volume of 1000 ml. The vessel is filled with 800 g of water and is continuously stirred. The reactor temperature is set to 20°C. When the reactor temperature is stable, the temperature difference between the jacketed and reactor is determined and kept constant during the experiment. This allows for isoperibolic operating conditions. The RSM which is placed inside the vessel is turned on for 30 s. The dissipated energy is calculated by  $P_{\text{diss}} = Mc_p\Delta T$ . For the inline RSM, two temperature probes of a Mettler Toledo EasyMax 102 Basic lab reactor are placed in the inlet and outlet tubes of the inline rotor stator mixer. The inlet and outlet tubes are placed at the same height to avoid additional flow due to gravity. The temperatures of the inlet and outlet flow are logged with an accuracy of 0.002°C (standard deviation on 100 data points) every 2 seconds until the temperature difference becomes constant. The temperature difference is corrected with the intrinsic temperature difference between the temperature probes. The inline RSM operates at different rotational speeds, which determines the free flow rate. Isoperibolic conditions are maintained by keeping the jacket of the RSM and the entering fluid temperature constant at 25°C. Additional temperature increase from the environment (RSM motor housing temperature) could lead to overestimation of the power draw. The power draw measurements are corrected with the offset of the power draw as a function of rotational speed.

## 2.4 Microencapsulation

Melamine formaldehyde prepolymer forms the continuous phase and silicone oil is used as dispersed phase. Table 1 shows the rheological properties of both liquids. The interfacial tension was measured

with a CAM 200 using the pendant droplet method. The oil to water phase ratio is kept constant at 42%. Both phases are pumped separately by peristaltic pumps (Watson & Marlow and Verder). The prepolymer is cooled to 10°C, to prevent reaction. The silicone oil is used at room temperature. Before entering the RSM, the two phases pass through an eight element Kenics® mixer with an internal diameter of 4.8 mm filling the mixing chamber and recycle loop with a polydisperse coarse emulsion with droplet diameters smaller than 2 mm. The jacket of the inline RSM is cooled with a thermostatic recirculation bath (Lauda Gold) and uses external temperature control to avoid temperatures inside the mixing chamber exceeding 40°C. The emulsion droplets are templates for the in situ microencapsulation process. 10 ml of the emulsion is collected in vials and the capsules are hardened at 80°C. The capsules are analysed using micrographs and image analysis software ImageJ (Abràmoff et al., 2004), resulting in number based capsule size distributions.

Table 1: Rheological properties of melamine formaldehyde prepolymer and silicone oil.

	Prepolymer	Silicone oil
Density (kg/m <sup>3</sup> )	1027	973
Viscosity (mPas)	13.5	337
Interfacial tension (mN/m)		24.3

### 3 Results and discussion

#### 3.1 Pumping capacity

The intrinsic flow rates of both inline and batch RSM are shown in Figure 3 as a function of rotational speed (rpm). The batch rotor stator mixer generates a flow rate several orders larger than the inline rotor stator mixer. For both batch and flow devices, the flow number ( $N_Q$ ) remains constant for the different rotational speeds and corresponding intrinsic flow rate. In the batch RSM,  $N_Q$  is 0.5, which is double the value of the high-end of the  $N_Q$  range (0.11-0.26) reported in literature for several RSM geometries (Håkansson, 2018). A good linear fit is found between the rotational speed and intrinsic flow rate up to 300 rpm. Towards the highest rotational speed the flow rate begins to deviate from the linear trend and begins to level off. For the inline RSM the flow number is 0.003, which is at the low end of the range mentioned in literature (0.002-0.08). As previously mentioned, flow rate in the inline RSM is restricted due to the housing around the mixing head and the narrow (4 mm) inlet and outlet tubes. In addition the large difference in flow number is also attributed to the geometrical differences between both devices. An increase in stator hole area and the number of leading edges gives more pumping capacity to the RSM (Paul et al., 2004). In the batch TG18 there are 12 leading edges and a total stator hole area of 2.88 cm<sup>2</sup> which is 18 times larger than the G2 stator hole area of the inline RSM.

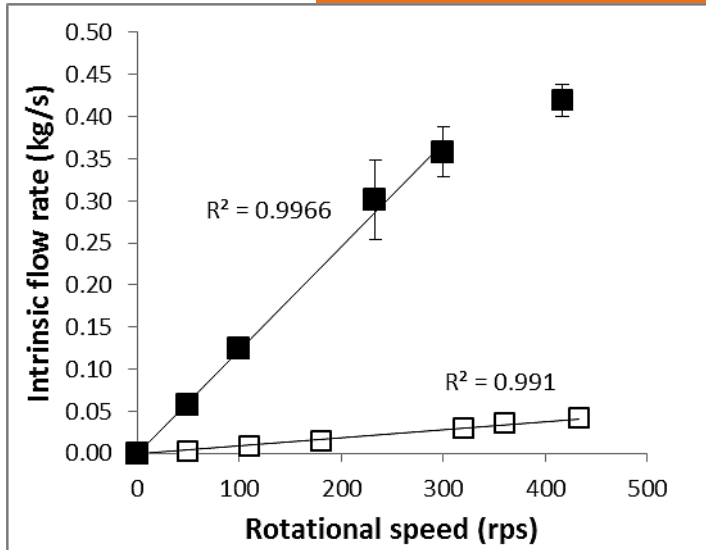


Figure 3: Intrinsic flow rate dependency on rotational speed in batch, ■, and inline RSM, □, (n=3).

### 3.2 Power draw

The relation between power draw and rotational speed is shown in Figure 4. A non-linear statistical modelling software program, Eureqa® (Nutonian), is used to find the best model to fit the data (Chen et al., 2018; Wieland and Rogasik, 2015). For both inline and batch RSM good correlations (Pearson correlation coefficient >0.995) are found with  $N$  to the power of 2.11 and 1.99 respectively. This indicates that the operating regime is laminar (Hall et al., 2011). The relation can be written as  $P_{\text{diss}} = C_7 N^2 D^2$ , whereby  $C_7$  is 2.39 for the batch RSM and 1.36 for the inline RSM. This indicates that the measured dissipated turbulent power is proportional to the total kinetic energy ( $N^2 D^2$ ). In stirred vessels this is known as the velocity head,  $H$ , which provides the shear in mixing through the jet or pulsating motion of the fluid and is dissipated by turbulence (Paul et al., 2004). This corresponds to the basic principle of the calorimetric measuring method used, whereby the turbulent dissipated energy is quantified through the amount of generated heat.

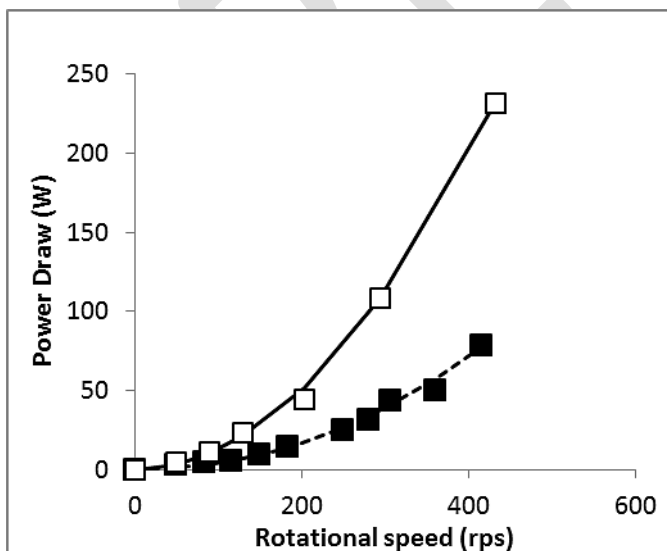


Figure 4: Power draw of inline □, and batch RSM, ■ measurement based on calorimetry and quadratic fits for inline (full line) and batch RSM (dotted line).

### 3.3 Transfer parameter

Tip speed, Weber number ( $We$ ) and energy density ( $E$ ) are explored as transfer parameters between the lab scale batch and pilot scale inline RSM. For an initial comparison the inline RSM is operated as close to batch mode as possible. Therefore the loop and mixing chamber are filled with coarse emulsion and the inlet and outlet are closed off. Weber number and energy density are explored using a low feed flow rate of 4g/min.

Figure 5 shows the mean volume based diameter ( $mean D_v$ ) and covariance for three tip speeds. The dotted lines indicate trends of capsule mean diameters obtained when a feed flow rate is introduced and is discussed in a later section. The residence time in the inline RSM is chosen to obtain equal energy densities as the batch RSM. It is clear that the inline RSM is unable to obtain the same mean diameter of microcapsules as in batch at equal tip speeds and energy density, and as a result these parameters are unable to transfer results from the batch to the inline device, when mean volume based capsule diameter is considered. The energy density is also a function of residence time (see equation 18), which in turn determines the number of passages. In the batch RSM at a tip speed of  $10 \text{ ms}^{-1}$  (rotational speed of 15000 rpm) the tank volume is recirculated 1.12 times per second, compared to 0.26 in the inline RSM. It is not possible to obtain the same number of rotations per second, therefore the total number of rotations is increased by increasing the residence time ( $>20 \text{ min}$ ) of the batch mode operated inline RSM. At equal turnovers and tip speed, the  $mean D_v$  decreases to some extent, but the  $mean D_v$  of the batch RSM is not matched. This indicates other factors (geometry, turbulent flow field) are influencing the droplet break-up. The fill ratio ( $F$ ), which characterises flow behaviour, of both devices is constant for the rotational speed range. The fill ratio of the batch RSM and the inline RSM were equal to 9% and 6%, respectively. This lower fill ratio in the inline module implies that the mixing is more likely to occur in the RSM clearance than the turbulent jets in the stator slots, making droplet break-up mechanistically different. Figure 5B shows the covariance of the volume based particle size distribution ( $CoV_v$ ). For both RSMs there is little influence of tip speed on the covariance of the distribution curves at the same number of turnovers.

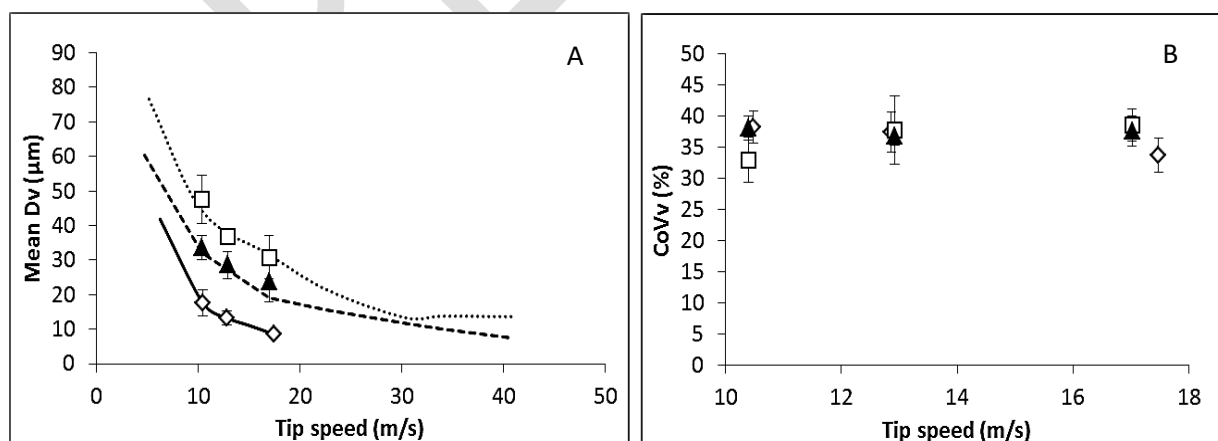


Figure 5: Dependency of volume based mean diameter and covariance on tip speed (A) and (B), respectively, in the batch and inline RSM. The inline RSM is operated without feed flow rate at two different residence times: 20 min residence time,  $\blacktriangle$  and 60 sec residence time,  $\square$ . Results obtained with the lab scale batch RSM are indicated by  $\circ$ . Each data point is the mean of three repetitions and error bars indicate the spread on these repetitions ( $n=3$ ). Trends of Inline RSM results at 4 g/min and 330 g/min feed flow rates are indicated by the striped and dotted line, respectively.

Figure 6 shows the mean  $D_v$  of both devices in function of the Weber number. The inline rotor stator mixer is operated with a feed flow rate of 4 g/min, ensuring similar number of turnover are obtained in batch and flow. There is again a different dependency of mean diameter on  $We$ , between the batch and inline device. Furthermore the CoV in the inline device shows no clear dependency on  $We$ , while the batch device shows a strong decline at Weber numbers below 20,000. This difference in covariance means the distribution curves differ in shape, which supports the hypothesis of different droplet break-up mechanisms in both devices.

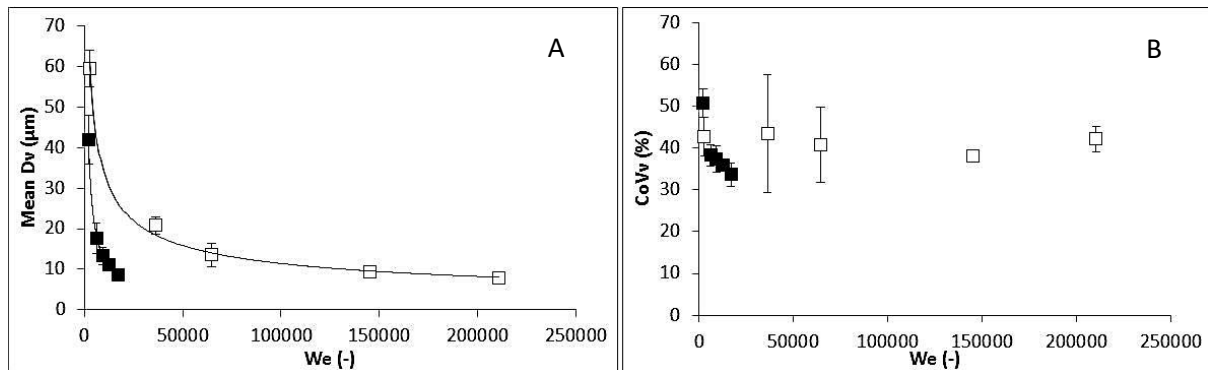


Figure 6: Dependency of volume based mean diameter and covariance on  $We$  for batch, ■ and inline RSM, □. Each data point is the average of three repetitions and error bars indicate the spread on these repetitions ( $n=3$ ).

### 3.4 Correlations for capsule diameter

As mentioned above, batch and inline mean  $D_v$  do not correlate with the Weber number.

Mechanistic models are usually based on maximum droplet diameters or the Sauter mean diameter, which are assumed to be proportional,  $D_{\max} \sim D_{32}$  (Paul et al., 2004). Figure 7 A presents the relation between the dimensionless maximum diameter, determined by the ratio of  $D_{95}$  and rotor diameter,  $D$ , to the Weber number. The inline RSM with recycle loop is operated with a low feed flow rate of 7 g/min. This feed flow rate ensures the same total residence time taking into account the average number of recirculations. The best correlation between  $D_{95}/D$  and  $We$  is found for an exponent of -0.4 on  $We$ . Hinze *et al.* (1955) related the maximum stable droplet in turbulent flow to  $We^{-0.6}$ . This larger exponent (-0.4) indicates a less efficient droplet break-up. The discrepancy with the Hinze model is to be expected as their model assumes inviscid droplets at low concentrations, which is not the case for the current conditions (Hinze, 1955). It is most likely that the viscous forces resisting droplet deformation, nor droplet coalescence can be ignored. With regard to the dimensionless maximum diameter the parameter  $We^{-0.4}$ , is an adequate transfer parameter. Figure 7 B, shows the results for the dimensionless Sauter mean diameter in function of  $We^{-0.4}$ . For the inline RSM, a good correlation is again found, while the results of the batch RSM are best fitted with a power equation with an exponent of 1.65, which leads to a correlation of  $D_{32}/D \sim We^{-0.66}$ . This comes close to the exponent of the Weber equation (-0.6) presented in equation 16.

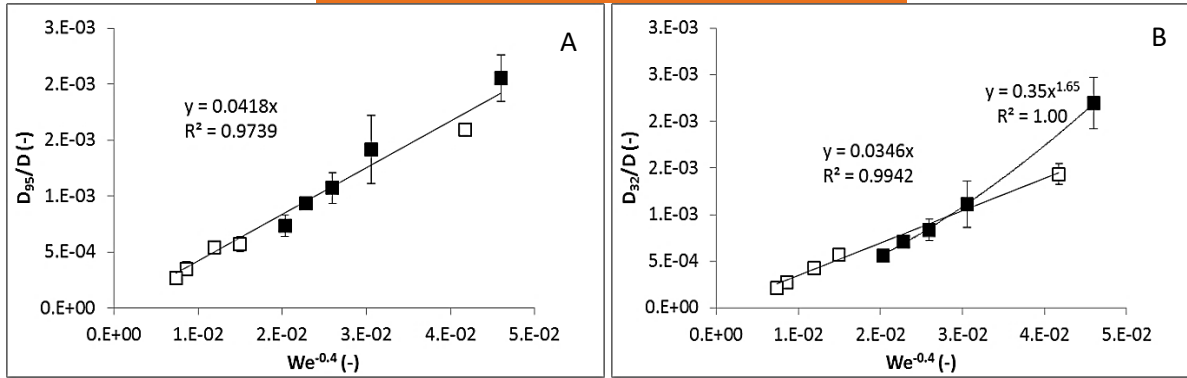


Figure 7: Dependency of dimensionless maximum diameter ( $D_{95}/D$ ) on Weber number for batch and inline RSM at equal residence time. Results are indicated by ■ for batch and □ for inline. Each data point is the average of three repetitions and error bars indicate the spread on these repetitions ( $n=3$ ).

Figure 8 shows the Sauter mean diameter in function of the energy density. Based on energy density, no correlation is found between batch and inline data. The exponents of -0.431 and -0.658 for the inline RSM and batch RSM, respectively, are consistent with the data found by Schubert *et al.* 2004, and indicate that the droplet size is dominated by inertial turbulent break-up in the inline RSM, while in the batch RSM turbulent shear gains importance (the exponent  $b$  of  $E$  is closer to -0.75) (Hall et al., 2011; Schubert and Engel, 2004).

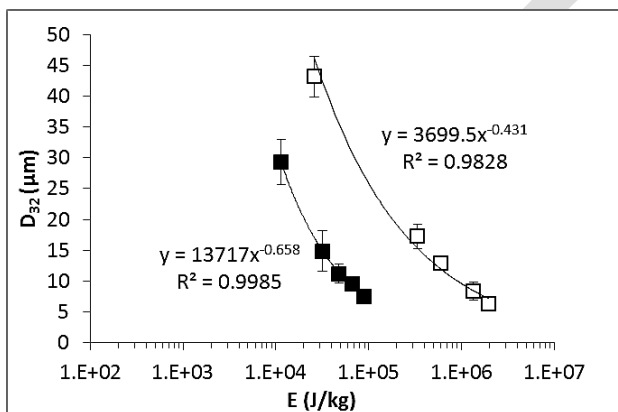


Figure 8: Dependency of Sauter mean diameter in energy density for batch, ■, and inline RSM, □, with equal residence times in the mixer head. The x-axis is presented by a logarithmic scale. Each data point is the average of three repetitions and error bars indicate the spread on these repetitions ( $n=3$ ).

### 3.5 Influence of feed flow rate

The inline RSM is operated at lab scale flow rates 4, 7 and 60 g/min and at increased flow rates of 120 g/min and 330 g/min, the latter feed flow rate can be considered production scale (20 L/h) for a microencapsulation process. The results are shown in function of tip speed, seen in Figure 9. It is clear that over the range of feed flow rates the mean diameters ( $D_v$  and  $D_n$ ) are very similar, there is a slight increase in mean diameters as the feed flow rate increases. This can be contributed to the difference in turnovers, which is shown in Figure 5. The trends of mean droplet diameter when a feed flow rate of 4 and 330 ml/min is applied, correspond well with the mean capsule size at high and low number of turnovers, respectively found in the batch operated inline RSM. At 4 ml/min the number of turnovers ( $Q_{intrinsic}/Q_{feed}$ ) are similar to batch and correspond to the results obtained with no feed flow rate and an extended residence time. As the feed flow rate increases, the number of turnovers decreases and mean diameters increase. The volume based covariance, shown in Figure

9B, stays between 30 and 50%. All volume and number based mean diameters and covariances are within a 30% and 20% interval, respectively, of the fitted trend through all the data points. These results indicate that this inline RSM can operate from lab scale to production scale, without the need to change equipment nor operating parameters. In addition, it shows that the efficiency of the inline RSM increases with increasing feed flow rate.

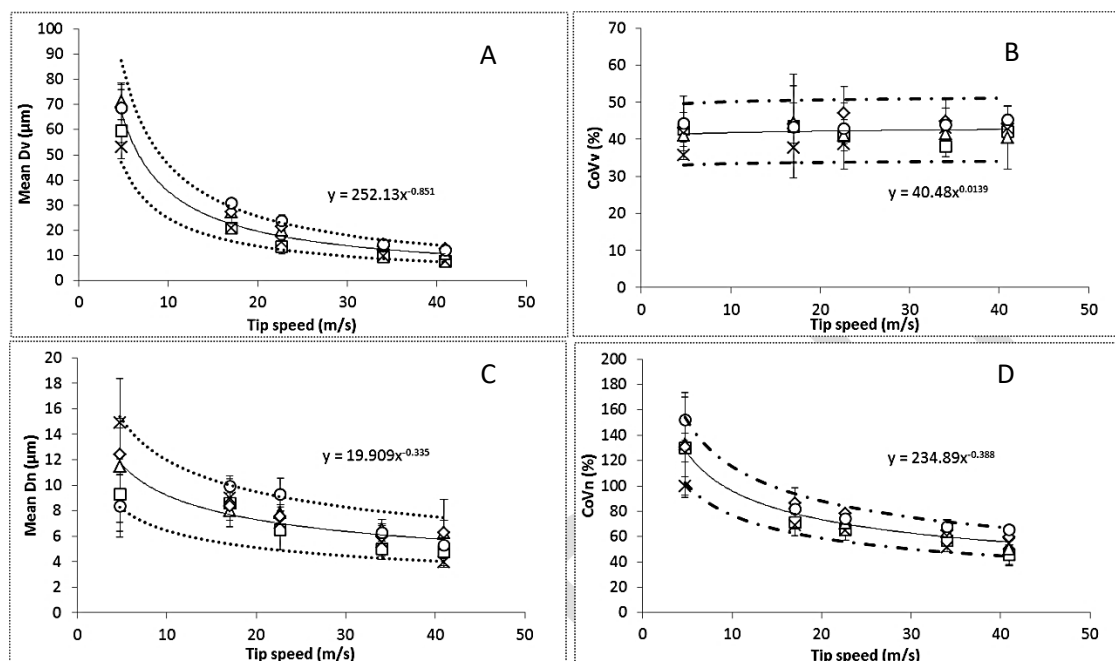


Figure 9: Influence of feed flow rate on volume and number based mean diameter (left) and covariance (right) in the inline RSM. Feed flow rates used are 4 g/min: □, 7 g/min: x, 60 g/min: Δ, 120 g/min: ◊, 330 g/min: ○. Solid lines indicate the general trend fitted through all data points, dotted lines indicate a 30% interval and dash dotted lines a 20% interval of the main trend. Each data point is the average of three repetitions and error bars indicate the spread on these repetitions (n=3).

#### 4 Conclusion

The emulsion generation for melamine formaldehyde microencapsulation using a batch lab scale RSM is compared to an inline pilot scale RSM. The inline RSM is implemented in a recycle loop, essentially a CSTR mode of operation, that allows the feed to pass multiple times through the mixing zone during continuous processing. Tip speed, energy density and Weber number were unable to correlate the mean volume based diameter of both batch and flow devices. Based on the difference in CoV it is assumed both devices present different droplet break-up regimes, which is attributed to the strong geometric differences of rotor and stator geometry. However the dimensionless maximum diameter, showed a good correlation with  $We^{-0.4}$ , for both devices working at a constant residence time. The CSTR mode of operation allows for feed flow rates to range from lab scale to pilot scale (330 g/min), within the same device and maintaining volume and number based mean diameter and covariance within a maximum 30% and 20% deviation, respectively, from the modelled trend. This promotes an alternative approach to scale-up. Lab scale development of encapsulation processes can be performed using an inline RSM with recycle loop leading to continuous processing at lab scale whereby scale-up of production is realised through the increase of the feed flow rate.

#### Declaration of interest

PREPRINT version. The formal article is published in Chemical Engineering and Processing - Process Intensification

<https://doi.org/10.1016/j.cep.2020.107989>

The authors declare that they have no known competing financial interests or personal relationships that could have appeared to influence the work reported in this paper.

### Acknowledgments

The author would like to thank Devan Chemicals for their support.

Funding: this work was performed with funding from the Agency for Innovation and Entrepreneurship and Catalisti grant number PIF HBC.2017.0442.

### References

- Abràmoff, M.D., Magalhães, P.J., Ram, S.J., 2004. Image processing with imageJ. *Biophotonics Int.* 11, 36–41. <https://doi.org/10.1117/1.3589100>
- Bansode, S.S., Banarjee, S.K., Gaikwad, D.D., Jadhav, S.L., Thorat, R.M., 2012. Microencapsulation : A Review. *Int. J. Pharm. Sci. Rev. Res.* 1, 509–531.
- Berkman, P.D., Calabrese, R. V., 1988. Dispersion of viscous liquids by turbulent flow in a static mixer. *AIChE J.* 34, 602–609. <https://doi.org/10.1002/aic.690340409>
- Calabrese, R. V., Wang, C.Y., Bryner, N.P., 1986. Drop breakup in turbulent stirred-tank contactors. Part I: Effect of Dispersed Phase Viscosity. *AIChE J.* 32, 677–681. <https://doi.org/10.1002/aic.690320418>
- Chen, C., Luo, C., Jiang, Z., 2018. A multilevel block building algorithm for fast modeling generalized separable systems. *Expert Syst. Appl.* 109, 25–34. <https://doi.org/10.1016/j.eswa.2018.05.021>
- Cohen, D., Ross, C., Company, S., 2005. Don ' t Fall Victim to. *Chem. Eng.* 6, 46–51.
- Cooke, M., Rodgers, T.L., Kowalski, A.J., 2011. Power Consumption Characteristics of an In-Line Silverson High Shear Mixer. *AIChE J.* 00, 1–10. <https://doi.org/10.1002/aic>
- El-hamouz, A., Cooke, M., Kowalski, A., Sharratt, P., 2009. Dispersion of silicone oil in water surfactant solution : Effect of impeller speed , oil viscosity and addition point on drop size distribution 48, 633–642. <https://doi.org/10.1016/j.cep.2008.07.008>
- Håkansson, A., 2018. Rotor-Stator Mixers : From Batch to Continuous Mode of Operation — A Review 1–17. <https://doi.org/10.3390/pr6040032>
- Håkansson, A., Arlov, D., Carlsson, F., Innings, F., 2017. Hydrodynamic difference between inline and batch operation of a rotor-stator mixer head - A CFD approach. *Can. J. Chem. Eng.* 95, 806–816. <https://doi.org/10.1002/cjce.22718>
- Håkansson, A., Innings, F., 2017. The dissipation rate of turbulent kinetic energy and its relation to pumping power in inline rotor-stator mixers. *Chmical Eng. Process.* 115, 46–55.
- Hall, S., Cooke, M., Pacek, A.W., Kowalski, A.J., Rothman, D., Engineering, C., Science, A., Manchester, M., Unilever, R., Ch, W., Hp, B., 2011. Scaling Up Of Silverson Rotor–Stator Mixers. *Can. J. Chem. Eng.* 89, 1040–1050. <https://doi.org/10.1002/cjce.20556>
- Hall, S., Pacek, A.W., Kowalski, A.J., Cooke, M., 2010. Emulsification by in-line rotor-stator mixers. *Conf. Pap.*
- Hall, S., Pacek, A.W., Kowalski, A.J., Cooke, M., Rothman, D., Unilever, R., Sunlight, P., 2013. The effect of scale and interfacial tension on liquid – liquid dispersion in in-line Silverson rotor –

PREPRINT version. The formal article is published in Chemical Engineering and Processing - Process Intensification

<https://doi.org/10.1016/j.cep.2020.107989>

stator mixers *Chem. Eng. Res. Des.* 91, 2156–2168.

<https://doi.org/10.1016/j.cherd.2013.04.021>

Hert, S.C. De, Rodgers, T.L., 2017. Continuous, recycle and batch emulsification kinetics using a high-shear mixer. *Chem. Eng. Sci.* 167, 265–277. <https://doi.org/10.1016/j.ces.2017.04.020>

Hinze, J., 1955. Fundamentals of the Hydrodynamic Mechanism of Splitting in Dispersion Processes 1, 289–295.

James, J., Cooke, M., Trinh, L., Hou, R., Martin, P., Kowalski, A., Rodgers, T.L., 2017. Scale-up of batch rotor–stator mixers. Part 1—power constants. *Chem. Eng. Res. Des.* 124, 313–320.

<https://doi.org/10.1016/j.cherd.2017.06.020>

Kamiya, T., Kaminoyama, M., 2010. Scale-Up Factor for Mean Drop Diameter in Batch Rotor – Stator Mixers 43, 326–332.

Karbstein, H., Schubert, H., 1995. Developments in the continuous mechanical production of oil-in-water macro-emulsions. *Chem. Eng. Process.* 34, 205–211.

Kowalski, A.J., 2009. An expression for the power consumption of in-line rotor-stator devices. *Chem. Eng. Process. Process Intensif.* 48, 581–585. <https://doi.org/10.1016/j.cep.2008.04.002>

Kowalski, A.J., Cooke, M., Hall, S., 2011. Expression for turbulent power draw of an in-line Silverson high shear mixer. *Chem. Eng. Sci.* 66, 241–249. <https://doi.org/10.1016/j.ces.2010.10.010>

Martin-Banderas, L., Ganán-Calvo, a. M., Fernández-Arevalo, M., 2010. Making Drops in Microencapsulation Processes. *Lett. Drug Des. Discov.* 7, 300–309.

<https://doi.org/10.2174/157018010790945760>

Pacek, A., Baker, M., Utomo, A.T., 2007. Characterisation of Flow Pattern in a Rotor Stator High Shear Mixer 1, 16–20.

Pacek, A.W., Hall, S., Cooke, M., Kowalski, A.J., 2013. Emulsification in Rotor-Stator mixers, in: *Emulsion Formation and Stability*. pp. 127–167. <https://doi.org/10.1002/9783527647941.ch5>

Paul, E.L., Atiemo-obeng, V. a, Kresta, S.M., 2004. HANDBOOK OF INDUSTRIAL MIXING. <https://doi.org/10.1002/0471451452>

Schubert, H., Engel, R., 2004. Product and formulation engineering of emulsions. *Chem. Eng. Res. Des.* 82, 1137–1143. <https://doi.org/10.1205/cerd.82.9.1137.44154>

Singh, M.N., Hemant, K.S.Y., Ram, M., Shivakumar, H.G., 2010. Microencapsulation: A promising technique for controlled drug delivery. *Res. Pharm. Sci.* 5, 65–77.

Wieland, R., Rogasik, H., 2015. Method for analyzing soil structure according to the size of structural elements. *Comput. Geosci.* 75, 96–102. <https://doi.org/10.1016/j.cageo.2014.11.007>